Selfconsistent domain theory in softferromagnetic media. III. Composite domain structures in thinfilm objects

H. A. M. van den Berg and A. H. J. van den Brandt

Citation: Journal of Applied Physics **62**, 1952 (1987); doi: 10.1063/1.339533
View online: http://dx.doi.org/10.1063/1.339533
View Table of Contents: http://scitation.aip.org/content/aip/journal/jap/62/5?ver=pdfcov
Published by the AIP Publishing

Self-consistent domain theory in soft-ferromagnetic media. III. Composite domain structures in thin-film objects

H. A. M. van den Berg and A. H. J. van den Brandt
Siemens Forschung Centrum, Postfach 3240, 8520 Erlangen, Federal Republic of Germany

(Received 10 September 1986; accepted for publication 10 April 1987)

The self-consistent domain theory, based on micromagnetic principles, is further developed in order to incorporate all possible solenoidal two-dimensional magnetization distributions in plane-parallel thin-film objects with arbitrary lateral shape. A decomposition of the object into a number of disjunct plane-parallel subregions that completely cover the object's area is put forward. In each subregion, a solenoidal **M** distribution is defined with the **M** vector parallel to the subregion's boundary, so that the **M** distributions in adjacent subregions properly link either via a continuous transition, or via a 180° wall at the intermediate boundary. Two types of subregions are distinguished; namely, the simple connected regions and the so-called parallel regions, being a special type of multiple connected region. In the first category, the basic structures as defined in the preceding paper on this subject are present. The parallel regions are closed ringlike configurations that are built of simpler units—the parallel segments. A parallel segment is a region bounded by two orthogonal trajectories of the same set of straight lines, while two of these straight lines close the segment at either end. No points of intersection of members of this family of lines are found inside the segment. In a specific parallel region, the distance between the orthogonal trajectories is the same for all segments. Adjacent segments in a parallel region are separated by a domain wall which is the locus of centers inside the cross section of the segments of circles that touch at corresponding orthogonal edges of both of the segments involved. A systematic procedure is developed for constructing the parallel subregions, and it is shown that, with this, all possible two-dimensional solenoidal **M** distributions can be recovered.

I. INTRODUCTION

The nonuniqueness in the domain structure in soft-ferromagnetic objects is a well-known phenomenon having already been recognized in the early childhood of domain theory; it has caused a lot of trouble for practical applications of these media. In this paper, we present a self-consistent theory based on micromagnetic principles, by which this multiplicity in the domain structure is predicted and from which all domain geometries possible can be extracted. We will not cover the general situation. First, we will deal with thin-film objects which are rectangular cylinders with plane parallel top and bottom surfaces and, second, with solenoidal two-dimensional dipole configurations in which the dipoles do not vary along the cylinder axis. The latter restriction implies that the external field and conduction currents are zero and that the medium possesses not a single bit of anisotropy.

Our approach is a further development of previous work[1,2] by van den Berg, in which the so-called basic domain structure, generally the simplest domain structure possible, was derived for thin-film objects with arbitrary lateral shape. In this paper, we shall lean heavily on the principles unfolded in the papers cited above, and therefore, only a brief recapitulation of the relevant basic ideas is in order.

It was shown[1] that the characteristic base curves of the partial differential equation governing the dipole distribution are straight lines in a one-to-one projection of the dipole distribution along the cylinder axis onto the bottom surface. Moreover, the magnetization is always perpendicular to these base curves, which, therefore, are perpendicular to the object edge. Ambiguities in the dipole direction arise at the intersections of the base curves with different orientations. The simplest domain configuration in a given object that prevents these ambiguities from occurring is the so-called basic structure. The extremities of the domain walls in the basic structure are either situated at free cluster knots (see Ref. 3, Chap. 4) or at the centers of curvature of convex parts of the edge where the radius of curvature is locally minimal. It was proven that the basic structure is the locus of the centers of all circles that, first, touch the object edge at at least, two points and, second, are completely situated within the object. This definition determines the basic structure uniquely in arbitrary objects; however, it is afflicted with some degree of arbitrariness in the case of multiple connected objects.[2]

In multiply connected objects, a decomposition of the object's area into so-called parallel subregions and concave simply connected subregions was put forward.[2] In each of these subregions, solenoidal distributions are defined, in which the dipoles are parallel to each subregion's edge, so that the various distributions do not mutually interfere. The edges of the parallel subregions are orthogonal trajectories of the same set of characteristic base curves (or two involutes of the same evolute) and are parallel to each other in the geodesic sense. It was shown that such a parallel region need not contain a single fragment of domain walls, so that, in general, these parallel dipole configurations are even simpler than the basic structures. In this paper, we shall hark back to this category of regions and shall generalize the concept of a

 0021-8979/87/171952-08$02.40

parallel region. Moreover, we shall further explore the idea of the object's decomposition into subregions in a systematic fashion.

II. DECOMPOSITION AND COMPLETENESS

In this paper, we aim at developing a procedure from which any domain structure possible in an arbitrary thin-film object can be derived. We pursue this completeness by decomposing the object into disjunct regions that cover the object completely, regions in which either basic structures or parallel configurations are defined. For this purpose, we shall examine in more detail the dipole distributions in domains.

A domain is a region which, first, is enclosed by either domain walls, or the object edge, or by domain walls and segments of the object edge, and second, in which any pair of points within the domain can be interconnected by a line that intersects neither domain walls nor the object edge. Note that, in general, the basic structure of an object is single domain in the above sense, although domain walls are present within the domain area. In the two-dimensional images, one single domain wall is a line either in between two centers of curvature with locally minimal radii of curvature corresponding to convex parts of the edge of subregions or the object, or in between one such center and a cluster knot or, finally, in between two cluster knots. Except at its extremity, no cluster knots are found on a wall.

In Fig. 1(a), such a domain with a continuous dipole distribution is given, so that the characteristic base curves, indicated by the thin straight lines, have no points of intersection. Moreover, the orthogonal trajectories of the base curves passing through the cluster knots A–E are given by the dashed curves. These trajectories divide the domain into disjunct regions 1 to 5, which completely cover the domain area. The distance between every pair of trajectories does not vary, because the magnetization is parallel to these lines and the **M** distribution is solenoidal. Thus, a specific width, denoted by the symbols b_1 to b_5, can be attributed to the regions 1–5 [see Fig. 1(a)]. Note that the width of region 1 is determined by the longest segment of the characteristics between the orthogonal trajectory through E and domain wall ED. A similar remark applies to region 5.

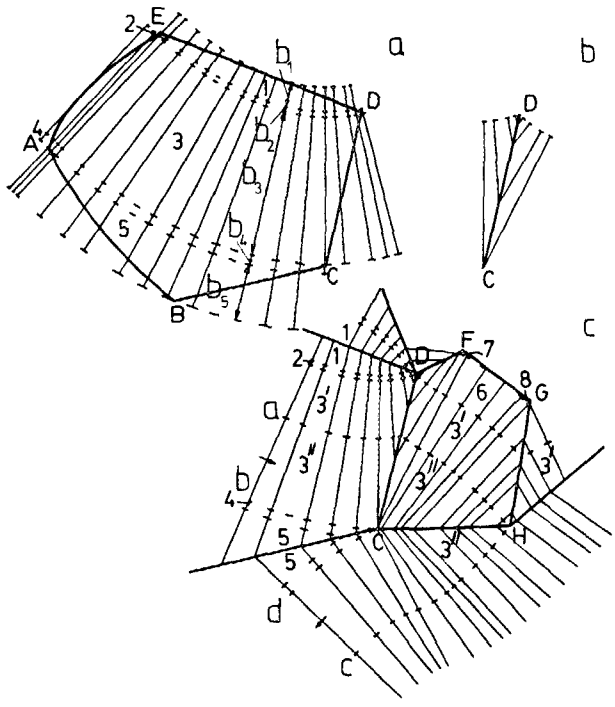

FIG. 1. (a) Decomposition of domain ABCDE into regions 1–5 bounded by orthogonal trajectories passing through the cluster knots A, C, D, and E. (b) Continuation of the regions 3 across domain-wall CD. (c) Further decomposition of region 3 by cluster knot H.

We examine the continuation of the orthogonal trajectories across a domain wall, i.e., the wall CD in Fig. 1(a) [see Fig. 1(b)]. At the domain walls the characteristics are subjected to the bisector relation, so that the width of the continuation of region 3 into the adjacent domain remains unchanged. Observe that the produced part of region 3 contains cluster knot H and, therefore, will be further split into regions 3′ and 3″ in order to avoid cluster knots within the regions. This division of region 3 is not confined to domain CDFGH; however, it also involves domain ABCDE and all other domains through which regions 3′ and 3″, or their subsequent decompositions, are crossing. Apart from the subdivision of 3, three extra regions 6, 7, and 8 are added in order to cover domain CDFGH's area. Region 6 is bounded by the trajectory through D and the trajectory touching at wall FG in order to keep the effective width constant, i.e., to prevent bifurcation of the **M** flux of subregions. Note that the decomposition is uniquely specified by the magnetization distribution in the domains and the geometry of the domain walls. By systematically incorporating all domains, we arrive at a unique decomposition of the object's area into subregions for the given magnetization distribution.

We consider more closely one such subregion, i.e., 3″. Assume that this region is not further subdivided by cluster knots; and, if not, we shall consider region 3‴ that satisfies this condition. In Fig. 1(c), we consider the segment abdc of 3″. At the characteristic through a and b, the dipole direction is as indicated in Fig. 1(c). Bearing in mind the Gaussian law, the condition $\nabla\cdot\mathbf{M} = 0$ and the parallelism of **M** to the orthogonal edges of 3″, it is obvious that the magnetization at the line cd is as indicated in Fig. 1(c). Evidently, line cd cannot coincide with the object edge, so there must exist another segment cdef of 3″ that meets segment abcd at line cd. Thus, line cd is replaced by ef; however, the above argument can be repeated for line ef, so that line ef is replaced by characteristic-base-line segment gh. An impeding expansion of the number of segments of 3″, and, along with this, an unbridled growth of 3″'s area can only be warded off by allowing line gh to coincide with line ab. In other words, 3″ and, thus, all subregions are bounded by two closed curves, being orthogonal trajectories of the characteristic base lines. We shall refer to these multiply connected regions with "parallel" edges as parallel (sub)regions.

Up to now, we have neglected the domains in which an isolated domain-wall configuration is present. Two situations have to be distinguished. In the first place, a completely isolated wall configuration is present within the domain [see Fig. 2(a)]. In this case, this wall configuration can be enclosed by an orthogonal trajectory of the characteristic base

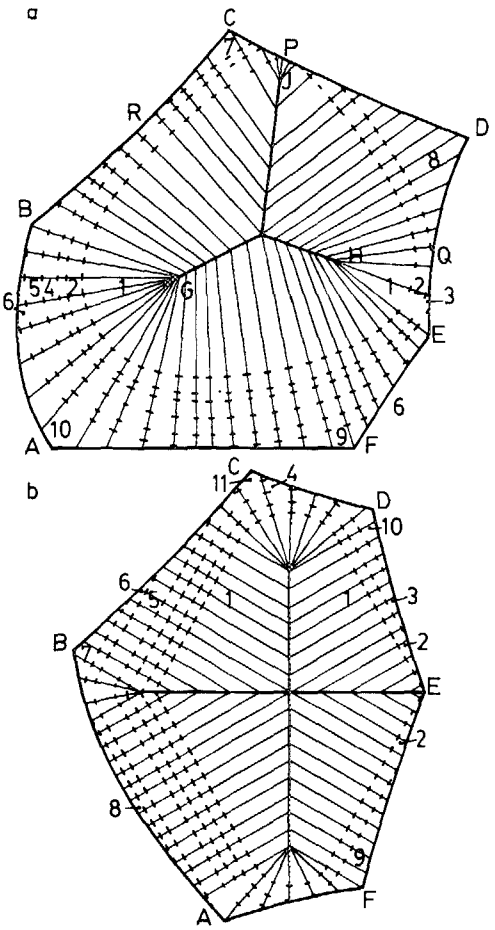

FIG. 2. Decomposition of domain ABCDEF with internal domain-wall structure. (a) Completely isolated wall configuration. (b) Internal wall configuration connected to the external one.

lines determining the magnetization distribution within the domain. In the second place, the interior wall configuration has one connection [knot E in Fig. 2(b)] with the exterior walls of the domain [AB, BC, CD, DE, EF, and FA in Fig. 2(b)]. (It can easily be seen that only one such interior wall structure is possible in each domain.) The decomposition proceeds as follows. Construct the orthogonal trajectory of the characteristic base curves that touches at the exterior walls of the domain without intersecting one of them [Fig. 2(a)] and, if this is not possible, the trajectory through the cluster knot that interconnects the internal wall structure with its external counterpart [Fig. 2(b)]. The trajectories obtained by this enclose region 1 in Figs. 2(a) and 2(b). Subsequently, a second trajectory is constructed within the domain that touches at the exterior wall next to the nearest of the above trajectory, and if this is not possible, the trajectory with its extremity at one of the cluster knots at that exterior wall is determined. This last step is repeated until the domain area is completely covered by subregions. Note that the basic structures of subregion 1 coincide with the internal wall configuration, or part of it, in Figs. 2(a) and 2(b), respectively. The other region, 2 to 11, form parts of parallel subregions for which a general procedure for the determination of the domain-wall positions will be developed in the course of this paper.

In conclusion, we may state that any object can be decomposed in a unique fashion for any possible domain configuration into disjunct subregions that completely cover the object area. These subregions are either simply connected and contain a basic domain configuration, or are parallel regions, which are multiply connected. The opposite should also hold. Any decomposition of the object into disjunct simply connected regions and parallel regions defines a valid domain structure. The definition of the domain configuration in simply connected subregions with arbitrary shapes was extensively discussed in the previous paper[2] and is unique. In this paper, we have to delve deeper into the parallel regions, in which two essential questions inflict themselves. First, the general procedure for generating all valid parallel regions must be outlined, and second, the dipole distribution in these regions must be determined. These questions will be the subject of Sec. III.

III. THE PARALLEL (SUB)REGIONS

In Sec. II, it has been demonstrated that the tangents to both edges of a parallel region are discontinuous at the domain wall that runs between these edge points of discontinuity. It appears that, in general, a parallel region is a combination of a number of segments. The definition of these basic segments—the parallel segments—will be the subject of Sec. III A.

A. Parallel segments and their coupling

A parallel segment is a region with a continuous magnetization distribution that is enclosed by two orthogonal trajectories of a family of straight characteristic base lines and two of these base curves at both ends [see Fig. 3(a)]. The

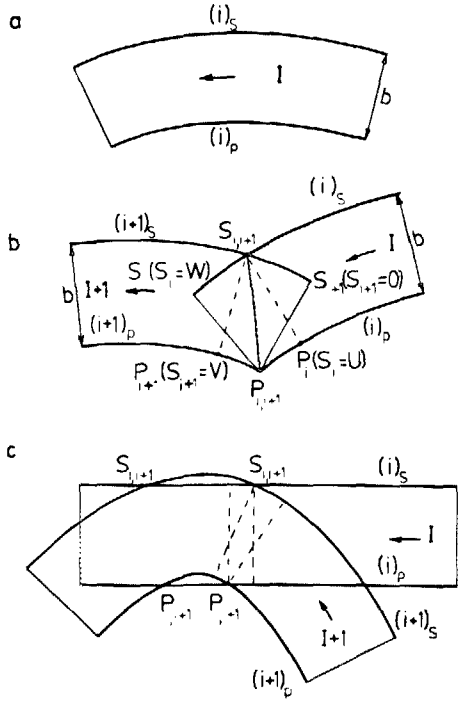

FIG. 3. (a) A parallel segment and the edge definition with respect to the orientation of the M flow, indicated by the arrow. (b) The domain wall between the parallel segments (i) and ($i+1$). (c) Two parallel segments with two pairs of points of intersection.

continuity of the **M** distribution implies that the radius of curvature of the convex parts of the orthogonal trajectories is always larger than or equal to the segment's width, i.e., the distance between the trajectories. By definition, we shall assume that a radius of curvature equal to the width can only occur at the extremities of the segments. It is self-evident that no restrictions result from this definition, because one can always put together two parallel segments whose exterior characteristic base lines coincide. To each segment, one of the two possible orientations of the **M** flow is attached. The bounding orthogonal trajectory to the right of an arbitrary **M** vector inside segment (i) is indicated by $(i)_s$, and its pendant by $(i)_p$ [see Fig. 3(a)]. Along the edges $(i)_p$ and $(i)_s$, a position parameter s_i is defined, such that complementary points $P(s_i = u)$ and $S(s_i = u)$ on edges $(i)_p$ and $(i)_s$, respectively, are situated at the same characteristic.

Now consider the coupling of two segments, i.e., (i) and $(i+1)$. Of course, these two segments form parts of a parallel (sub)region, in which the **M** flow is either clockwise or anticlockwise. The segments are consecutively numbered from (i) to (n) in compliance with the circulation direction of the **M** flow. We require that the pair of segment edges $(i)_p$ and $(i+1)_p$ and the pair $(i)_s$ and $(i+1)_s$ both have at least one point of intersection. Obviously, the distances between the edges $(i)_s$ and $(i)_p$ and between $(i+1)_s$ and $(i+1)_p$ are equal. We shall consider the situation in which each edge pair, to wit, $(i)_p$ and $(i+1)_p$ and the pair $(i)_s$ and $(i+1)_s$, has one point of intersection, marked by $P_{i,i+1}$ and $S_{i,i+1}$, respectively.

Again, a domain wall must take care of matching the dipole configurations in segments (i) and $(i+1)$. Of course, one of the extremities of this wall has to be situated at the point of intersection of the segment edges where the center of curvature is on the inside of the parallel subregion [$P_{i,i+1}$ in Fig. 3(b)], because characteristic base curves that originate at the segment edges on either side of the above point of intersection [edges $(i)_p$ and $(i+1)_p$ in Fig. 3(b)] intersect inside the parallel subregion. From the theory developed in the preceding paper,[2] it can easily be seen that this domain wall is the locus of centers, inside the parallel region, of circles that touch at both edges $(i)_p$ and $(i+1)_p$ in our example. Note that point $S_{i,i+1} = S_i(s_i = u) = S_{i+1}(s_{i+1} = v)$ is the center of the circle that touches at $P_{i+1}(s_{i+1} = v)$ and $P_i(s_i = u)$ and, therefore, constitutes the other extremity of the domain wall. It is obvious that this domain wall is governed only by the segments $P_{i,i+1}P_i$ $(s_i = u)$ and $P_{i,i+1}P_{i+1}(s_{i+1} = v)$ of edges $(i)_p$ and $(i+1)_p$, respectively.

The complementary points of $P_{i,i+1} = P_i(s_i = w) = P_{i+1}(s_{i+1} = 0)$ at edges $(i)_s$ and $(i+1)_s$ are S_i $(s_i = w)$ and $S_{i+1}(s_{i+1} = 0)$, respectively. The locus of centers of circles that touch at both segments $S_{i,i+1}S_i$ $(s_i = w)$ and at $S_{i,i+1}S_{i+1}(s_{i+1} = 0)$ coincides with the already-established domain wall.

Note that a special situation presents itself when the pair of edges $(i)_s$ and $(i+1)_s$ are touching at $S_{i,i+1}$. In this case, edges $(i)_p$ and $(i+1)_p$ will touch in the complementary point of $S_{i,i+1}$, and a continuous transition between both parallel segments exist.

We have confined ourselves to two parallel segments of which corresponding edges have only one point in common. An example of the opposite situation is provided in Fig. 3(c). Pairs of points of intersection of corresponding edges can be distinguished, namely $S_{i,i+1}$ and $P_{i,i+1}$ and the pair $S'_{i,i+1}$ and $P'_{i,i+1}$. $S_{i,i+1}$ and $P_{i,i+1}$ can be recognized as a pair, because the complementary points of $P_{i,i+1}$ at edges $(i)_s$ and $(i+1)_s$ are situated on both sides of $S_{i,i+1}$ and vice versa. Observe that the points of intersection need not arise in pairs for the exterior points of intersection. The question that arises is whether the domain walls that can be constructed between all these pairs are of any significance. Bear in mind the previously defined consecutive numbering of the parallel segments. By definition, the domain wall between the following pair is selected to serve as boundary between segments (i) and $(i+1)$: the complete pair of points of intersection that is first met when, starting from the domain wall between segments $(i-1)$ and (i), segments (i) and $(i+1)$ are traced along the circulation direction of **M**. Of course, two successive parallel segments are only properly defined when such a pair of points of intersection exists.

We have currently confined ourselves to the coupling of two adjacent parallel segments. However, in general, a complete parallel subregion consists of many segments. The definition of these segments is subjected to limits as we shall see. Consider the three adjacent segments (1) to (3) (see Fig. 4). As stated previously, the sequence in the numbers refers to the sequence of segments that is consecutively met when tracing the parallel subregions along the **M** direction. Of course, the same order has to exist in the domain walls that separate the various parallel segments. This implies that the edge points $S_{2,3}$ and $P_{2,3}$ must exist and lie on the proper side of $S_{1,2}$ and $P_{1,2}$, respectively (on the left side in Fig. 4). Moreover, the domain wall between $S_{1,2}$ and $P_{1,2}$ and the one between $S_{2,3}$ and $P_{2,3}$ are not allowed to intersect. In the Appendix, it is shown that this requirement is satisfied when the edge segment between $S_{2,3}$ and $S_3(s_3 = w)$ (see Fig. 4), the wall shape codefining part of edge (3), does not intersect the edge segment between $S_1(s_1 = v)$ and $S_{1,2}$, which codetermines the shape of the wall in between segments (1) and (2). Note that the above limitation to edge $(3)_s$ implies that the edge segment between $P_{2,3}$ and $P_3(s_3 = x)$ does not intersect the edge segment between $P_{1,2}$ and $P_1(s_1 = y)$. This relationship should, of course, also be expected for symmetry reasons. Bearing in mind the above restriction, we can extend the number of elements at will.

A last aspect, however, should be kept in mind. We denote that part of the parallel segment (i) in between the domain wall between $S_{i-1,i}$ and $P_{i-1,i}$, and the one between $S_{i,i+1}$ and $P_{i,i+1}$, by π_i. The following should apply:

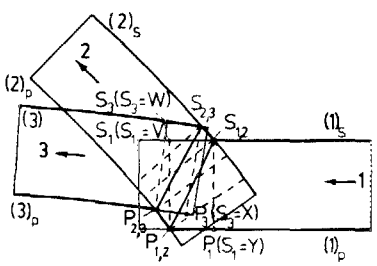

FIG. 4. Three successive parallel segments and a number of significant edge points.

$\pi_1 \cap \pi_2 \cap \ldots \cap \pi_n = 0$, in which n is the total number of segments in the parallel subregion.

B. Special couplings between parallel segments

In Sec. III A, we have encountered two different types of couplings; first, the continuous mode in the event that the corresponding pairs of edges of adjacent parallel segments are touching, and second, the mode in which one single domain wall interconnects both points of intersection of corresponding edges of the adjacent segments. One may wonder whether the combination of one point of intersection and one point of contact is possible. In principle, the answer is affirmative; however, in this case, we shall decompose the subregion into two parallel subregions, one with a coupling of the first type and the other one with an intermediate wall. Of course, this procedure does not give rise to any loss in generality.

We return to Fig. 1(a) and, in particular, to the cluster knot C. In point C, three domain walls of the parallel subregion 3 meet. This situation, in which domain walls of a number of parallel regions share one of their extremities, will be systematically explored.

In Fig. 5, the p edges of a number of parallel segments have point P in common. We present a systematic reconstruction of this configuration. First, we combine the segments (1) and (2) whose edges intersect at P and $S_{1,2}$. To trace the course of M at P, the M direction along edge $(i)_p$ at P will be denoted by β_i, where $0 \leqslant \beta_i < 2\pi$. This angle may vary between 0 and 2π. Again, as shown in the Appendix, segment $S_{2,3}S_3(s_3 = w)$ does not intersect segment $S_{1,2}S_1(s = u)$ for a feasible coupling of the segments. Note that the angle $\beta_{1,3} = \beta_3 - \beta_1 + \pi$ is always larger than π [watch the mutual positions of $S_1(s_1 = u)$ and $S_3(s_3 = w)$ in Fig. 5(b)]. For a proper course of the domain wall in between segments (3) and (4), segment $S_{3,4}S_4(s_4 = x)$ does not intersect its counterpart $S_{1,2}S_2(s_2 = v)$. Note that $\beta_{1,4}$ varies in between $\beta_{1,2}$ and 2π and might be smaller than π. These observations indicate that the angle $\beta_{1,m}$ is always larger than π when m is odd, and between zero and 2π when m is even. The correctness of this expectation is confirmed by the so-called corner cluster relations.[4]

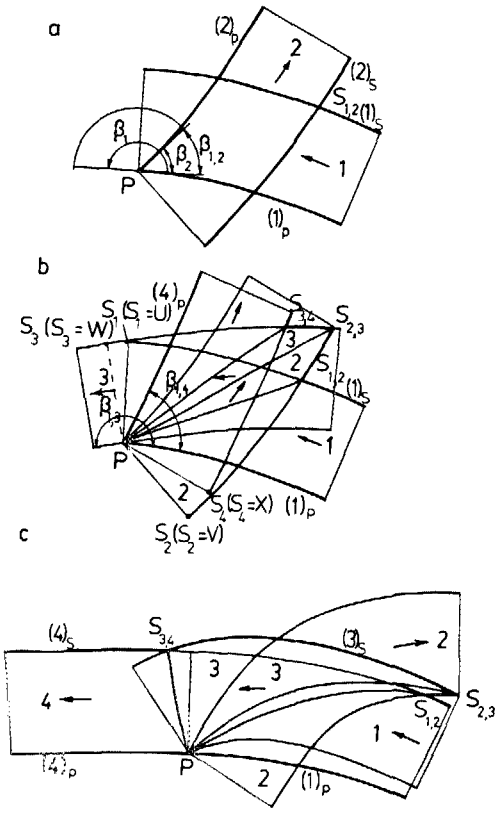

FIG. 5. Special types of segment coupling.

The situation in which $\beta_{1m} = \pi$, i.e., when edge $(1)_p$ produces $(M)_p$, deserves special attention. The edge-cluster relations[5] yield m's which must be even because M must be parallel in the exterior parallel segments (exterior domains in the cluster terminology). An example with $\beta_{1,m} = \pi$ is given in Fig. 5(c). Observe that we are restricted in the choice of the parallel segments because of the assumption $\beta_{1,m} = \pi$. (Observe that the basic structures in simply connected regions can also be derived by combining parallel segments, so that these segments can be conceived of as the basic elements in solenoidal magnetization distributions. On the other hand, the basic structure is a concept that can more easily be handled, so that it will be maintained for practical reasons.)

IV. DISCUSSION

We now recapitulate the main findings of this paper. We have introduced a decomposition of the object's area into a number of disjunct subregions that completely cover the object. Two different types of subregions have been distinguished; first, simply connected subregions in which the basic domain structures are present, and second, the multiply connected parallel regions with their associated dipole distributions. It has been shown that any solenoidal two-dimensional M distribution possible in thin-film objects can be described in terms of united subregions with either basic or parallel configurations. Therefore, a general procedure by which any parallel subregions can be constructed suffices to cover all dipole configurations possible.

The starting point in this construction is the parallel segment. A parallel segment is bounded by two orthogonal trajectories to the M-vector field, and, at each end, by one characteristic base line. The trajectories have continuous directional derivatives, and measured along the characteristic base curves, the edges have constant distance—the segment width. A parallel subregion is a combination of overlapping parallel segments with equal width that constitute a ring-shaped closed configuration. Two adjacent segments are either coupled by one domain wall that interconnects the points of intersection of corresponding trajectories, or a continuous transition exists in case trajectories of both segments touch pair wise. The various segment-separating domain walls cannot intersect each other and can only have their extremities in common. In the latter case, regions arise that, at first glance, can hardly be recognized as parallel regions (see Fig. 6).

During the construction of the parallel configurations, we have assumed a specific circulation sense of M. It is ob-

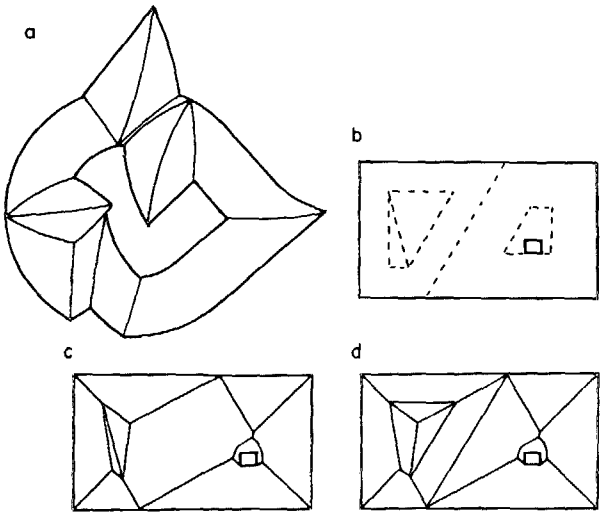

FIG. 6. (a) Example of a parallel subregion and the required domain walls. (b) Decomposition of the object into subregions. (c) and (d) Two of the domain structures that correspond with decomposition (b).

vious that the ultimate shape of the parallel subregion and its domain-wall configuration are equally valid when the circulation sense is the opposite. Similarly, the basic wall configuration in simply connected subregions does not depend on the circulation sense. On the other hand, a 180° wall has to arise at the intermediate boundary between adjacent subregions with opposite M on both sides of the intermediate boundary, so that the domain-wall configuration is positively affected by the circulation senses in the various subregions. Given only the shapes of the n subregions in which the object is decomposed, 2^{n-1} different domain-wall configurations are possible. A few examples are provided in Figs. 6(b)–6(d), where two of the 16 possible configurations are shown.

As mentioned in Sec. I, composite domain structures are frequently met in practice, not only in thin-film objects[3,6–13] but also in soft-magnetic whiskers.[14–19] In Fig. 7, simple examples of composite structures in permalloy elements and their corresponding decompositions into merely simply connected subregions are given. Note that the specimen in Fig. 7(c), with a thickness of 700 Å, contains two cross ties and that the M distribution is not perfectly solenoidal. Similar crosses can be observed in the domain structure of Fig. 8(a); however, this time, edge triplets are present to match the continuation of the M distribution near the cross with the boundary condition at the edge. Observe that two parallel subregions turn up [see Fig. 8(b)]. Details of very complex structures were presented by DeBlois.[10–13] An interpretation of Fig. 11 of Ref. 11 and of Fig. 32 of Ref. 10 is given in Figs. 8(c) and 8(d), respectively, in order to demonstrate the validity of the procedure presented for specimens in which the impact of the anisotropy is distinctly visible.

A brief discussion of DeBlois'[10] broad view of the order in the domain structure is necessary. He defined topological diagrams involving a number of closed loops in the domain structure along which there is flux closure. It is self-evident that these closed loops bear resemblance to the parallel subregions. On the other hand, in general, each DeBlois loop contains a number of parallel and simply connected subregions. Moreover, DeBlois' approach is meant as a schematic analytic tool and is not an attempt to predict the possible domain-wall configurations in his rectangular thin-film objects.

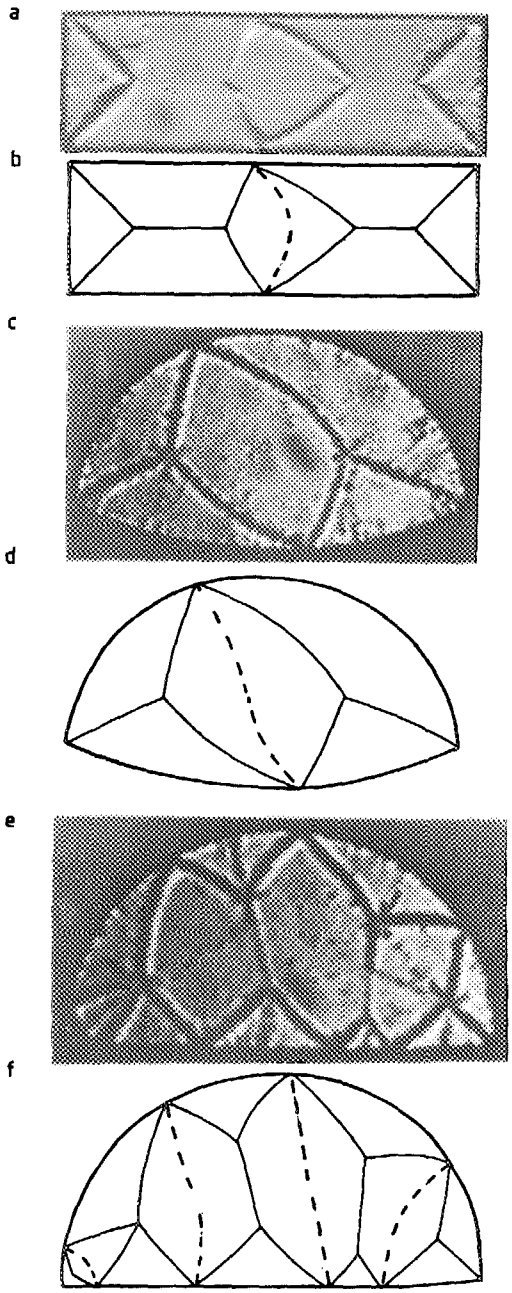

FIG. 7. Domain structures in permalloy elements and their interpretation in terms of a decomposition into disjunct subregions with basic domain structures. (a) Rectangular bar ($60\times20\,\mu$m). (b) Object bounded by circle segments (length: $60\,\mu$m). (c) Object bounded by circle segment and straight line (length: $60\,\mu$m).

Up to now, no attention has been paid to the impact of the wall and the anisotropy energy. These energies will certainly be different for the various domain structures in a given sample. In an element with small lateral dimensions, there is a tendency towards domain structures with a minimal wall length, i.e., towards basic structures in simply con-

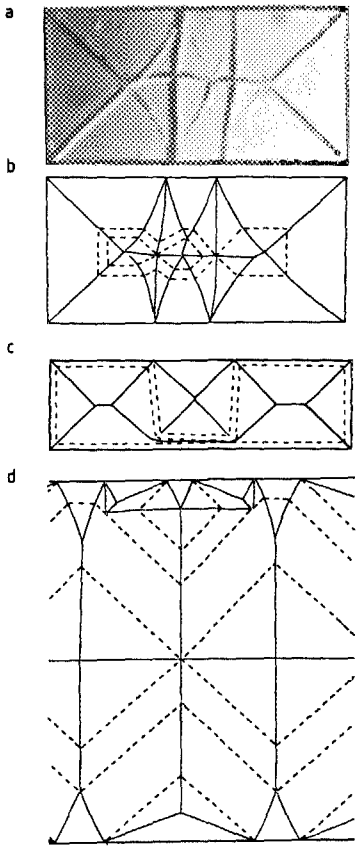

FIG. 8. A composite domain structure with parallel subregions. (a) Permalloy bar ($60\times30\ \mu$m). (b) Interpretation of configuration in (a). (c) Interpretation of domain structure of Fig. (11) of General Electric Report, no. 65-C-082 (1965), by R. W. DeBlois. (d) Interpretation of domain structure of Fig. (32) of General Electric Report, no. AFCRL-68-0414 (1968), by R. W. DeBlois.

nected objects. This can be explained as follows. Given a certain lateral shape, the wall and the anisotropy energy are a linear and a quadratic function of the linear scaling factor of the lateral dimensions, respectively. Therefore, the anisotropy energy will dominate in objects with large lateral dimensions, and thus, tends to enforce complex structures in order to reduce the area of domains with an unsuitable **M** distribution. An example is given in Fig. 9, in which a cubic anisotropy with an easy axis along the diagonals of the square is assumed. For small lateral dimensions, the basic structure of Fig. 9(c) will have the minimal energy. When the lateral dimensions grow, the domain structures of Figs. 9(a) and 9(b) are more likely.

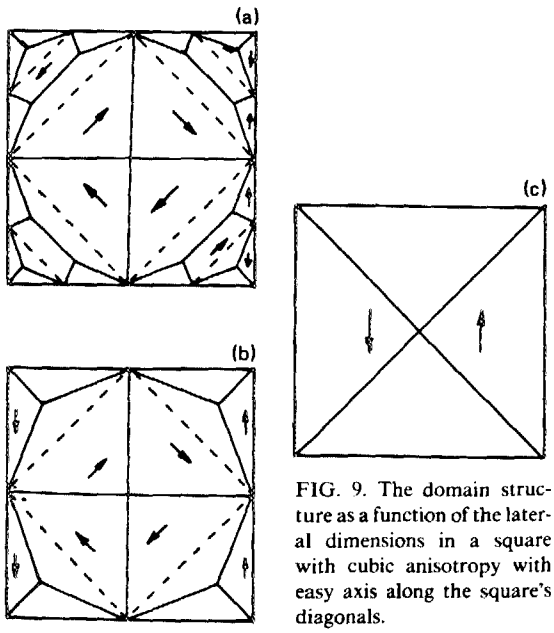

FIG. 9. The domain structure as a function of the lateral dimensions in a square with cubic anisotropy with easy axis along the square's diagonals.

It should be emphasized that whether or not these minimal energy configurations will arise depends strongly on the prehistory of the **M** distrbution and the presence of defects. It has been experimentally observed[20,21] that relatively small defects can enforce the domain structure to develop itself towards deviating higher-energy states. However, these configurations are again composite structures and can be derived from the theory presented.

ACKNOWLEDGMENT

The authors wish to thank J. B. van Staden for preparing the samples.

APPENDIX

We consider three successive parallel segments (1)–(3) and investigate whether there are restrictions on their shapes and mutual positions. In Sec. III A, the only requirement from the mutual positions of two adjacent segments (1) and (2) is the existence of two points of intersections $S_{1,2}$ and $P_{1,2}$. The course of the separating domain wall between (1) and (2) is governed by the edge segments $S_{1,2}S_1(s_1 = u_2)$ and $S_{1,2}S_2(s_2 = v_2)$ at edges $(1)_s$ and $(2)_s$, respectively, or, equivalently, by edge segments $P_{1,2}P_1(s_1 = u_1)$ and $P_{1,2}P_2(s_2 = v_1)$ [see Fig. A 1(a)]. Even so, the domain wall between the parallel segments (2) and (3) is governed by the

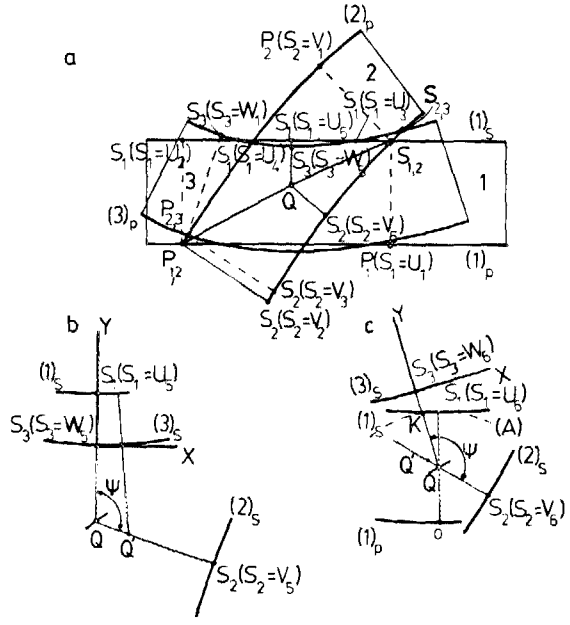

FIG. A1. (a) Three successive parallel segments (1)–(3), and the wall-shape-determining edge segments. (b) Construction when edge (3), is on the wrong side of edge $(1)_s$. (c) Construction when edge (3), is on the right side of edge $(1)_s$.

edge segments $S_{2,3}S_2(s_2 = v_3)$ and $S_{2,3}S_3(s_3 = w_1)$. The position of $P_{2,3}$ at edge $(2)_p$ with respect to $P_{1,2}$ has to comply with the course of **M** along the edge and the numbering of the segments. The same applies to the position of $S_{2,3}$. The fulfillment of these requirements is considered to be a prerequisite.

However, in addition, the domain wall between $P_{2,3}$ and $S_{2,3}$ must not intersect the one between $P_{1,2}$ and $S_{1,2}$. We shall prove that this requirement is satisfied when the domain-wall codetermining part of edge $(3)_s$, $S_{2,3}S_3(s_3 = w_1)$ does not intersect the domain-wall codetermining part of edge (1_s), $S_{1,2}S_1(s_1 = u_2)$.

First, investigate the situation in which $(1)_s$ and $(3)_s$ intersect at the points $S_1(s_1 = u_4)$ and $S_1(s_1 = u_3)$. By virtue of the continuity of the tangents to edges of the segments, it can be concluded that there exists a point at $(1)_s$, i.e., $S_1(s_1 = u_5)$, where the characteristic base curves of the parallel segments (1) and (3) coincide. This base line intersects the domain wall between segments (1) and (2) at Q, where the distance $|S_1(s_1 = u_5)Q| = |S_2(s_2 = v_5)Q|$. It is obvious that $|S_3(s_3 = w_5)Q| < |S_1(s_1 = u_5)Q|$. Look for the position of the points of the domain wall between segments (2) and (3) at the base line through $S_2(s_2 = v_5)$. The points of intersection of the latter base line with the characteristics of (3) will be called Q'. We erect a Cartesian coordinate system with its origin at $S_3(s_3 = w_5)$ and a y axis along the base curve through $S_1(s_1 = u_5)$ [see Fig. A1(b)], while the positive x axis is on the side where the angle Ψ between the characteristics at Q is smaller than π. At a sufficiently small x, the edge $(3)_s$ can be approximated by the quadratic relation $y = ax^2$ with $|a| < 1/(2b)$, where b is the segment width. In a first-order approximation, the difference in distance of Q' from edges $(1)_s$ and $(3)_s$ as a function of x decreases by

$$[(1 - \cos\Psi)/\sin\Psi][1 + 2a|S_3(s_3 = w_5)Q|]x.$$

Observe that $(1 - \cos\Psi)/\sin\Psi$ is larger than zero because $0 \leqslant \Psi \leqslant \pi$, and that

$$[1 + 2a|S_3(s_3 = w_5)Q|] > 0$$

since

$$|2a| < 1/b \quad \text{and} \quad |S_3(s_3 = w_5)Q| < b.$$

As a result, the absolute value of the mutual difference in the distance of Q' from edges $(1)_s$ and $(3)_s$ decreases for positive x. It is obvious that Q' moves towards edge (2_s). This tendency is also preserved at large x, because the base lines of parallel segment (3) do not intersect each other inside (3). Therefore, the ultimate Q' at the domain wall between segments (2) and (3) is on the wrong side of the domain wall between segments (1) and (2).

Subsequently, we attempt to prove that all points of the wall between segments (2) and (3) are correctly situated with respect to the wall between points $S_{1,2}$ and $P_{1,2}$ when edge segments $S_{2,3}S_3(s_3 = w_1)$ and $S_{1,2}S_1(s_1 = u_2)$ do not intersect. In Fig. A1(c), the domain-wall point Q at the characteristic base lines through $S_1(s_1 = u_6)$ and $S_2(s_2 = v_6)$ is indicated. The circle (A) with radius b, where b is the segment width, touches at segment edge $(1)_s$ at $S_1(s_1 = u_6)$. Observed from Q, the base curve corresponding to $S_3(s_3 = w_6)$ will consecutively intersect circle A, edge $(1)_s$, and finally, $(3)_s$. Bearing in mind that the distance $|S_1(s_1 = u_6)Q| < b$, it follows from simple geometrical considerations that $|QK| \geqslant |S_1(s_1 = u_6)Q|$, so that $|S_3(s_3 = w_6)Q| > |QK| \geqslant |S_2(s_2 = v_6)$ [see Fig. A1(c)].

After having established this fact, we erect a Cartesian coordinate system with its center at $S_3(s_3 = w_6)$, with the y axis along the base line through $S_3(s_3 = w_6)$ and with its positive x axis pointing towards the side where the angle Ψ between the characteristics through $S_3(s_3 = w_6)$ and $S_2(s_2 = v_6)$ is smaller than π. We can now repeat the arguments employed in the previous case. It can be seen for very small x that the distance $|Q'S_2(s_2 = v_6)|$ becomes closer to the distance between Q' and edge $(3)_s$ when moving toward the negative x direction. As a consequence, Q' moves apart from $S_2(s_2 = v_6)$ when x becomes more negative. This tendency is continued at large negative x values because the characteristic base lines of segment (3) do not intersect inside this segment. Thus, if present, the point of the domain wall between the segments (2) and (3) on the base curve through $S_2(s_2 = v_6)$ is found and is at the correct side of the wall in between $P_{1,2}$ and $S_{1,2}$. Note that when edge segment $S_{2,3}S_3(s_3 = w_1)$ does not intersect edge segment $S_{1,2}S_1(s_1 = u_2)$, their counterparts at edges $(3)_p$ and $(1)_p$, respectively, will likewise not intersect. We have also assumed that $P_{1,2}$ and $P_{2,3}$ are different points. It is obvious that the same conclusions apply when $P_{1,2}$ and $P_{2,3}$ coincide.

[1] H. A. M. van den Berg, J. Appl. Phys. **57**, 2168 (1985).
[2] H. A. M. van den Berg, J. Appl. Phys. **60**, 1104 (1986).
[3] H. A. M. van den Berg, Ph.D. thesis (Delft University of Technology, Delft, The Netherlands, 1984).
[4] H. A. M. van den Berg, J. Appl. Phys. **54**, 4512 (1983).
[5] H. A. M. van den Berg and D. K. Vatvani, J. Appl. Phys. **52**, 6830 (1981).
[6] S. R. Herd, K. Y. Ahn, and S. M. Kane, IEEE Trans. Magn. **MAG-15**, 1824 (1979).
[7] G. W. Garnett and W. D. Corner, J. Magn. Magn. Mater. **30**, 11 (1982).
[8] Y. Nakamura, K. Yamakawa, and S. Ivasaki, IEEE Trans. Magn. **MAG-21**, 1578 (1985).
[9] A. Hubert, J. Magn. Magn. Mater. **35**, 249 (1983).
[10] R. W. DeBlois, General Electric Report, No. AFCRL-68-0414 (1968).
[11] R. W. DeBlois, General Electric Report, No. 65-C-082 (1965).
[12] R. W. DeBlois, J. Appl. Phys. **36**, 1647 (1965).
[13] R. W. DeBlois, J. Appl. Phys. **39**, 442 (1968).
[14] R. W. DeBlois and C. D. Graham, J. Appl. Phys. **29**, 528 (1958).
[15] R. W. DeBlois and C. D. Graham, J. Appl. Phys. **29**, 931 (1958).
[16] R. V. Coleman and G. G. Scott, Phys. Rev. **107**, 1276 (1957).
[17] R. V. Coleman and G. G. Scott, J. Appl. Phys. **29**, 526 (1958).
[18] G. G. Scott and R. V. Coleman, J. Appl. Phys. **28**, 1512 (1957).
[19] L. Drewello and H. H. Mende, J. Magn. Magn. Mater. **13**, 231 (1979).
[20] H. A. M. van den Berg and F. A. N. van der Voort, IEEE Trans. Magn. **MAG-21**, 1936 (1985).
[21] F. A. N. van der Voort and H. A. M. van den Berg, Proc. E. Mater. Res. Soc. Conf. 1986, **41** (1986).